Analytical Methods

Accepted Manuscript

This article can be cited before page numbers have been issued, to do this please use: R. Escudero, M. Cabral, M. Valladares, M. Franco and R. Pérez, *Anal. Methods*, 2020, DOI: 10.1039/C9AY02183C.

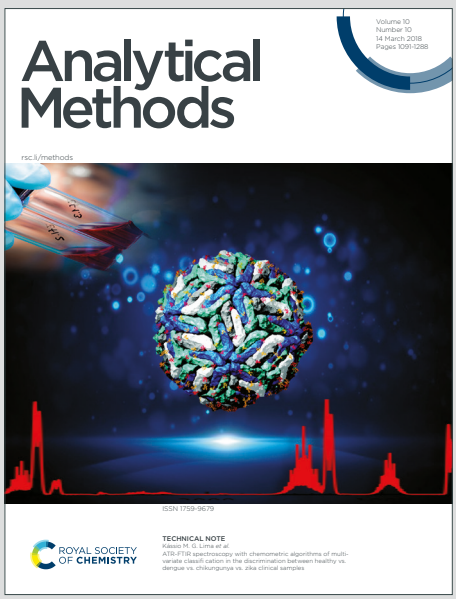

ROYAL SOCIETY OF CHEMISTRY

rsc.li/methods

View Article Online
DOI: 10.1039/C9AY02183C

ARTICLE

Received 00th January 20xx,

Accepted 00th January 20xx

DOI: 10.1039/x0xx00000x

Breast cancer analysis by confocal energy dispersive micro-XRD

Rodrigo O. Escudero,*[a] María C. Cabral, [b] Mariana Valladares, [b] María A. Franco, [b] and Roberto Daniel Perez [a,c]

In this work, confocal energy dispersive micro-XRD technique has been employed to efficiently study differences between normal and malignant carcinomas in breast tissues. This technique has been implemented with low angular divergence glass monocapillaries in the excitation and detection channels. The microdiffractometer operates with a scattering angle of (20.3 ± 0.9)º that defines a cross section for analysis (0.178mm×0.175mm), with a depth resolution of 1.18mm. The obtained momentum transfer resolution between 3.9-10.9% was found to be highly useful to identify scattering profiles of adipose tissues without any data processing. Differentiation between tissues with similar scattering profiles, such as fibroglandular and neoplastic tissues, has been achieved by processing the spectra within the framework of diffraction theory for scattering intensity. The obtained results allowed the developing of a deterministic diagnostic model based on the evaluation of the depth profiles analysis by confocal micro-XRD. In this model, the modulation of the scattering profiles caused by x-ray attenuation was analyzed to differentiate neoplastic tissues. The spatial resolution of the technique was the key aspect of the process, helping to detect variations in x-ray attenuation and to select uniform volume of analysis without superimposed scattering profiles.

Introduction

At a global scale, breast cancer is one of the highest incidence diseases for women's health. Currently, mammography is the technique most commonly used to initially identify abnormal tissues in breast. The benign or malignant character of neoplasms cannot be determined by conventional mammography. Therefore, a biopsy is usually done through extracting suspicious tissue and analysing it in a histological laboratory. When the biopsy corresponds to a benign neoplasm, the sample mostly consist in woven fibroglandular, a particular mixture of connective and glandular tissue that can have a low percentage of adipose tissue[1]. Differently, the biopsies classified as carcinomas may have areas composed of normal tissues (fibrous, glandular or adipose), which highlights the need of a microscopic analysis to diagnose the disease[1].

Traditionally, analysis of biopsies is performed by a histopathologist who has wide experience on the subject product of several years of training. The incorporation of additional instrumental techniques that complement the traditional analysis can be remarkably helpful, both for technical staffs training and for the veracity of the diagnoses made. Within the possible instrumental techniques, X-Ray Diffraction Analysis (XRD) stands out, due to its ability to efficiently differentiate biological breast tissue (adipose, fibroglandular and neoplastic)[2-4]. The accuracy of the classification decreases considerably when the tissue is inhomogeneous because of the overlap caused by the diffraction spectra belonging to different molecular structures[5]. X-Ray Microdiffraction (micro-XRD) solves this problem allowing to select the analysis area with micrometric spatial resolution[5,6].

Using either reflection or transmission geometries, Micro-XRD technique can be implemented. However, transmission geometry is more suitable, since it has smaller beam path into the sample minimizing heterogeneity effects on the scattering intensity[6]. In this geometry, the absorption of the radiation significantly affects the shape of the scattering profiles. This effect can be used to classify neoplastic tissues, since they have linear attenuation coefficients slightly higher than normal tissues[7]. However, knowledge of the sample thickness is essential to efficiently compare the radiation absorption of different tissues. This represents a great challenge, especially for analysing amorphous samples of biological tissues by micro-XRD. On this subject, it is complicated to achieve direct measurement of the samples thickness and detection of radiation paths, through micrometric cross section of these beams. Confocal micro-XRD in energy dispersive configuration can be employed to solve this issue[8].

Confocal setup extends the spatial resolution of the x-ray microanalysis into the depth, with the help of x-ray optics. The foci of two lenses, one in the excitation channel and the other in the detection channel, defines a micro-volume for probing the sample. Fluorescence and scattered radiation, ideally, are

[a] IFEG (Physics Institute Enrique Gaviola), CONICET (National Research Council Scientific and Technical) Córdoba, Argentina.
[b] Pathological Anatomy Service. Maternal Provincial Hospital Dr. Raúl Felipe Lucini. Córdoba, Argentina.
[c] Faculty of Mathematics, Physics, Astronomy and Computation. National University of Córdoba. Córdoba Argentina.
See DOI: 10.1039/x0xx00000x

View Article Online
DOI: 10.1039/C9AY02183C

detected only from this volume. This setup is proved to be capable of supplying depth-sensitive information on the composition of a sample with a minimum spatial resolution of 10 micrometers. The usefulness of the new 3D micro-XRD method has already been shown at several applications[9-11].

This paper describes the development of an energy dispersive confocal micro-XRD spectrometer and a procedure for classifying mammary biopsies, to be used in the diagnosis of breast cancer. The device consists of an experimental arrangement in confocal geometry that takes advantage of the variation in the x-ray attenuation of different types of breast tissues, helping with an efficient discrimination of its scattering spectra.

Experimental

Basic principles of micro-XRD

The energy dispersive micro-XRD combines the Energy Dispersive X-Ray Diffraction (EDXRD) with the spatial resolution of the x-ray microanalysis. EDXRD is a well-known method which can be implemented without complex mechanical devices to move the detector or source, considering that the scattering angle is fixed. This method takes advantage of the high energy resolution of semiconductor x-ray detectors technology to electronically scan in energy the scattered beam, looking for constructive interference peaks. In the case of crystals, these peaks originate from coherent scattering in the different atomic planes according to Bragg's condition:

$$d[\text{Å}] = \frac{6.199}{E[keV]\sin\theta} = \frac{1}{2q}[\text{Å}] \qquad (1)$$

where d is the interplanar spacing of the lattice planes in angstroms (Å), 2θ is the scattering angle, E is energy of the scattered photons in keV and q is the momentum transfer. Hence, the energy of any particular diffraction peak depends upon the scattering angle. Particularly, this angle is tuned in such a way that the diffraction peaks of interest fall in the useful range of x-ray flux available from the source being used[12]. The Full Width at Half Maximum (FWHM) of a diffraction peak (ΔE_{FWHM}) depends upon the angular resolution of the system ($\Delta\theta$) and the energy resolution of the detector (ΔE_D). For a single peak, the ΔE_{FWHM} can be taken as the minimum energy separation between two resolved diffraction peaks, i.e. as a measure of the ability of the system to resolve the peaks in momentum transfer space (momentum transfer resolution, $\Delta q/q$). The d-spacing resolution ($\Delta d/d=\Delta q/q$) can be estimated from $\Delta\theta$ and ΔE_D by means of statistical error propagation derived from the equation (1):

$$\left(\frac{\Delta d}{d}\right)^2 = (\Delta\theta\, ctg\theta)^2 + \left(\frac{\Delta E_D}{E}\right)^2 \qquad (2)$$

Here, the energy variation is mainly caused by the $(\Delta E_D)^2$ which for solid state detectors has a linear dependence with E[12]. As an example, for the x-ray detector Si-PIN Moxtek XPIN-XT employed in this work it is:

$$\Delta E_D^2[keV^2] = 0.00889 \times (E[keV] - 5.89) + 0.0404$$

Confocal setup for micro-XRD

To implement the energy dispersive confocal setup is required two x-ray lenses: one to focus the incident x-rays and the other to collect scattered radiation, as shown in Figure 1. The intersection of the foci of both lenses determines the volume of analysis whose dimensions can be accurately known by precharacterization of the lenses used. In this arrangement is important to use x-ray lenses with very low angular divergence in order to introduce low dispersion at angle 2θ. If the focus of each lens is described by a probability distribution, then the compound probability calculated as the product of both distributions describes the spatial sensitivity of the spectrometer. The confocal volume is defined by the level curve where the height of this composed probability reduced to $e^{-1/2}$ of its value at the maximum. Following the mathematical description provided by Kanngießer and Malzer[8], it takes the geometric figure of a paraboloid. If a set of orthogonal axis is settled as in Figure 1, then this level curve intersects the axis at:

$$\sigma_x = \frac{\sqrt{\left(\sigma_T^2 + (\cos(2\theta)\sigma_0)^2\right)}}{\sin(2\theta)}; \quad \sigma_y = \frac{\sigma_0\sigma_T}{\sqrt{\left(\sigma_T^2 + (\cos(2\theta)\sigma_0)^2\right)}};$$

$$\sigma_z = \frac{\sigma_0\sigma_T}{\sqrt{(\sigma_0^2 + \sigma_T^2)}} \qquad (3)$$

The x coordinate is along the symmetry axis of the focusing lens and the z coordinate is perpendicular to the dispersive plane which contains the excitation and detected beams. In the last equation, σ_0 is the focus size of the focusing lens and σ_T is the focus size of the collecting lens.

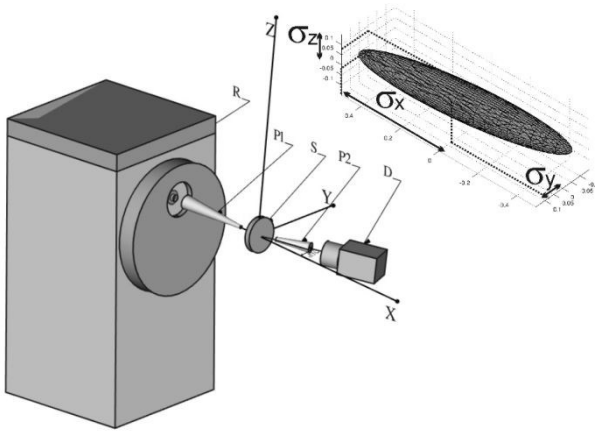

Figure 1: Experimental setup used for the implementation of the micro-XRD technique. In this figure, R is the diffraction x-ray tube with Mo anode, P1 and P2 are the input and output conical monocapillaries, respectively, S is the sample and D is the Moxtek Si-pin x-ray detector. In the upper right corner there is a graphical representation of the confocal volume showing the parameters σ_x, σ_y and σ_z.

View Article Online
DOI: 10.1039/C9AY02187C

For depth profile analysis, it is only employed the cross section of the confocal volume along the incident beam. When the center of the confocal volume is placed at $x = 0$ it is given by:

$$\eta(x) = \frac{\eta_0}{\sqrt{2\pi}\sigma_x} e^{-\frac{x^2}{2\sigma_x^2}} \quad (4)$$

Here η_0 is a proportional constant related to the x-ray transmission of both lenses. This function usually is called sensitivity of the confocal spectrometer for depth profile studies[8].

For a layer sample of thickness t with its incidence surface at $x = 0$, the intensity of coherent scattering at energy E when the center of the confocal volume is in the position x can be calculated from:

$$I(x) = \eta_0 I_0 e^{-\frac{\mu t}{\cos 2\theta}} e^{\frac{(\mu\alpha\sigma_x)^2}{2}} e^{\mu\alpha x} \delta \frac{d\sigma_c}{d\Omega} \Delta\Omega \, D(x) \quad (5)$$

Here, I_0 is the intensity of the incident beam at energy E, μ is the linear attenuation coefficient of the sample at energy E, α is a parameter defined by $\alpha = (1/\cos(2\theta)) - 1$, δ is the number of atoms or molecules per unit of volume, $d\sigma_c/d\Omega$ is the differential cross section of coherent scattering by atom or molecule at energy E, $\Delta\Omega$ is the solid angle subtended by the lens in the detection channel and $D(x)$ is a function defined by:

$$D(x) = \frac{1}{2}\left[erf\left(\frac{(\mu\alpha\sigma_x^2 + x)}{\sqrt{2}\sigma_x}\right) - erf\left(\frac{(\mu\alpha\sigma_x^2 + x - t)}{\sqrt{2}\sigma_x}\right)\right] \quad (6)$$

Here, *erf* is the error function.

The XRD spectra of mammary tissue have two main peaks that must be registered precisely: a peak associated with adipose tissue ($q \cong 1.1\text{nm}^{-1}$) and the other with the fibrous tissue ($q \cong 1.65\text{nm}^{-1}$)[13]. To improve the efficiency in the identification of these tissues, the scattering angle 2θ should be chosen so that the energy of the scattered photons in both peaks was below the 20keV. This condition ensures that the differences between the attenuation coefficients of the different types of mammary tissues can be detected more clearly. For the developed spectrometer was projected $2\theta = 20º$, so the energy of the scattered photons in the main fatty peak should be around 7.7keV and in the fibrous at 11.6keV.

Instrumentation

3 kW Mo x-ray tube Philips model PW2275/20 with a long fine focus oriented as a point source was used in the experiments. The Mo anode was in the horizontal plane with a focus dimension of 0.4 mm × 12 mm. The direction of the maximum intensity of the x-ray beam pointed down at 6º from the horizontal plane. It is the ideal orientation for the lens axis that optimizes the input photon flux on the lens. From this direction the x-ray source looks as a point source of 0.4mm×1.26mm area.

For the implementation of the confocal micro-XRD setup were used two conical monocapillaries with thick glass walls that minimize spurious signals[14]. The beams transmitted by these lenses have very low angular divergence so they introduce low dispersion at angle 2θ. For the excitation channel the capillary had a length of 130mm, inlet diameter d_{in} = 0.8 mm and output diameter d_{out} = 0.3 mm. Its input was 50mm far from the point source of the x-ray tube. For the detection channel the capillary had a length of 25mm, d_{in} = 0.45 mm and d_{out} = 0.55 mm. The distance from the intersection of both lens axis to the tip of the excitation lens was 3mm and to the tip of the detection lens was 6mm. The x-ray detector was placed at 5mm from the output of the second lens. Lenses were aligned using commercial manuals positioners Newport model Cat.LP-05A. The excitation channel lens was aligned without the presence of the second lens magnifying the copper XRF signal coming from a 2 micron thick copper foil. To align the second lens was magnified the maximum of the copper XRF signal recorded in successive copper foil scans along the direction of the incident beam. Figure 2 displays the scan corresponding to the optimal alignment of the confocal arrangement. By fitting the Gaussian model of the sensitivity (equation (4)) the value σ_x = (0.50 ± 0.01) mm was obtained. Conventional knife-edge scan were used to determine the lateral dimensions of the confocal volume giving σ_y = (0.076 ± 0.004) mm and σ_z = (0.075 ± 0.005) mm. By taking the FWHM of the orthogonal projections of the confocal volume was possible to calculate the volume of analysis as (0.178mm×0.175mm×1.18mm).

The sample was placed using a motorized sample holder controlled by a computer with a spatial resolution of 13 microns for the three orthogonal directions. X-rays were collected with a Si-PIN detector Moxtek XPIN-XT. The detector efficiency was determined by a Montecarlo simulation using the software PENELOPE[15] with input data delivered by MOXTEK. Between 4keV and 12keV the efficiency was greater than 90%. For energies greater than 12keV the efficiency showed a gradual decay. As an example the efficiency at 12 keV was 93.87% and for Mo-Kα line (17.44keV) was 60%.

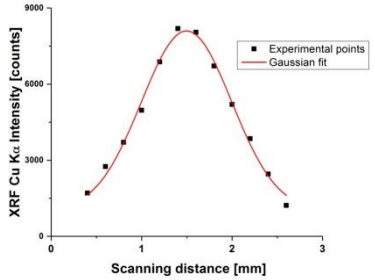

Figure 2: XRF emission of a 2 micron Cu foil scanned along the incident beam using the aligned confocal setup.

Resolution of the microdiffractometer

Once both lenses were arranged in an efficient excitation-detection configuration, the scattering angle 2θ was determined. It was achieved by measuring the x-ray scattering of a reference standard of silicon powder (NIST SRM640c) with

an average granulometry of 4.9 micron. For this material the most intense Bragg reflection corresponds to the atomic planes (111) with interplanar spacing of 0.31350nm. The powdered silicon was placed in a plastic cylinder of 10 mm in diameter and 1 mm in height and its bases were closed with a film of Kapton 8 microns thickness (SPEX Inc.). The cylinder was arranged so that the x-ray beam would have a normal impact on its bases. A spatial scan of the x-ray diffraction was performed by displacing the sample along the direction of the incident beam. In this way the position of the maximum dispersion was determined, which was then used to take several XRD spectra. Ten XRD spectra were taken rotating the sample around the direction of incidence to avoid alterations of the scattering profile caused by the focused excitation beam[5]. The average of the 10 recorded spectra is shown in the Figure 3. The scattering angle obtained from this average spectrum was 2θ = (20.3º ± 0.9º). The resolution of the microdiffractometer at 11.2 keV obtained as described in Theory subsection was 5.3%. For the energy range [5 keV, 16 keV] used in this work the resolution was enclosed between 10.9% and 3.9%. In particular, for the energy of the adipose peak (7.7 keV) the resolution was 6.9%, while for the fibrous peak (11.6 keV) was 4.9%. According to equation (1) and (2) the angular resolution was Δθ = 8mrad = 0.46º.

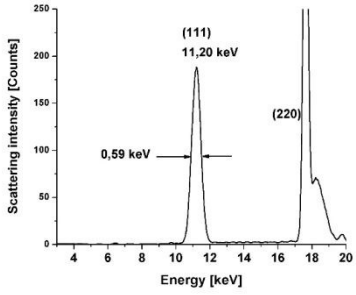

Figure 3: XRD spectrum for pulverized silicon NIST SRM640c obtained with the micro-XRD confocal spectrometer. The Bragg reflection (111) was used to calculate the momentum resolution. The graph also shows a strong Bragg reflection (220) that has been increased by the contribution of Mo-Kα line.

Measurement of thickness sample

The proposed procedure to determine the thickness of breast tissue samples based on confocal setup consisted on the scanning of the sample in depth. The step of this scan was 0.1mm and the acquisition time per point was 60s. It was tested by analyzing phantoms of PMMA because this material presents x-ray attenuation similar to biological tissues. Four plates of PMMA of 1, 2, 3 and 4 millimeters of thickness were analyzed. The scattering intensity in the confocal setup given by equation (5) was fit to the experimental scan for the Mo-Kα line. The comparison of the values measured with caliber and with the proposed method is shown in Table 1.

Caliber thickness [mm]	Confocal thickness [mm]
1.00 ± 0.01	1.03 ± 0.05
2.00 ± 0.01	1.99 ± 0.05
3.00 ± 0.01	3.05 ± 0.08
4.00 ± 0.01	4.0 ± 0.1

Table 1: Measurements of the thickness of PMMA phantoms by caliber and using the confocal micro-XRD setup.

Confocal micro-XRD in breast tissues

For the purpose of obtaining comparable scattering spectra, it was necessary to place the confocal volume in an easily reproducible position. In this work the position chosen produced the maximum intensity for the coherent scattering of the Mo-Kα line. It was achieved by a depth profile analysis scanning the confocal volume through the sample. Since all breast samples were cut with an approximately thickness of t = 2mm, it was a good approximation to consider that the maximum intensity I_{max} of the coherent scattering occurs at $x = t/2$ in such a way that:

$$I_{max} = \eta_0 I_0 e^{-\frac{\mu t}{\cos 2\theta}} e^{\frac{\mu a t}{2}} \delta \frac{d\sigma_c}{d\Omega} \Delta\Omega \, \mathrm{D_{max}} \qquad (7)$$

Here, D_{max} is the maximum of the function D. The scattering profiles of the tissue samples were obtained setting the x-ray tube at 40kV-20mA with an acquisition time of 1800s.

As was mentioned in the Introduction, the scattering profiles are superimposed to the XRF emission. In the analysis of breast tissues with this particular spectrometer, only Ca and Fe traces at energies far from the main scattering peaks were detected. For this reason, the XRF emission was not relevant in the data analysis of scattering patterns.

Breast tissue samples

A total of 35 samples of breast tissue were analyzed with the microdiffractometer, 15 of them were classified as normal, 5 as adipose tissue and the remainder as ductal carcinomas. All samples were obtained from patients submitted to surgical breast reduction mammoplasties and prophylactic mastectomies or quadrantectomies at Maternal Provincial Hospital Dr. Raúl Felipe Lucini of the Province of Córdoba, Argentina. After surgery, the extracted material were fixed and preserved at room temperature in 10% formaldehyde. Later, a sample of 2 mm thick was cut with a freezing microtome for measuring by micro-XRD. A second sample was cut in the adjacent tissue at 2 micrometer thick and then was stained with Hematoxylin-Eosin to identify the tissues in three histological categories: adipose, glandular and ductal carcinomas. The collection and handling of breast biopsy samples were carried out in accordance with the requirements of the Ethics and Training and Teaching Committee of the Hospital.

The first step of sample preparation for micro-XRD analysis consisted on removing the excess of formalin by running

water. After that the sample rested for 10 minutes to drain the water. The goal was to remove the excess of liquid because it increases the x-ray attenuation of the incident and emergent beams affecting the micro-XRD spectrum of the sample. The effect of formaldehyde at low concentrations was not significant in the confocal micro-XRD analysis which agrees with previous reports[16]. This was concluded after making a comparison between the spectra of pure water and formalin measuring, under the same conditions with the spectrometer. These liquid samples were placed in the same sample holder used for the reference standard of silicon powder employed in the study of the resolution of the microdiffractometer.

To irradiate the sample, it was placed in a plastic cylindrical sample holder of 34 mm in diameter and 2mm in height with its bases closed by an 8 micron thick Kapton film. The cylinder was attached to the automatic holder with their bases perpendicular to the excitation beam. To select the irradiation points the 2 micrometer thick adjacent section of the sample was carefully observed with the optical microscope in order to identify homogeneous areas. Using a webcam placed inside the sample chamber of the spectrometer, these areas were recognized in the irradiated sample to be then analyzed by confocal micro-XRD.

Results and discussions

Figure 4 shows the scattering profiles for adipose, fibroglandular and ductal carcinoma, respectively. The pattern of the adipose tissue was clearly distinguished from the others without any data processing. However, the scattering profiles of fibroglandular and ductal carcinoma are quite similar, both showing a prominent peak at the same value of the momentum transfer (around 1.65 nm^{-1}). For samples with equal thickness, this scattering peak is slightly smaller in malignant tumors due to the higher x-ray attenuation of neoplastic tissues. Variations in x-ray attenuation can also be employed to distinguish both types of tissues even when the sample thickness is not constant. In this case the scattering profiles are modulated by the exponential decay factors shows in equation (7). To characterize this modulation the rate between the scattering fluxes at two different momentum transfer can be used. For an efficient characterization, the gap between the energies of the scattering photons should be enough to clearly observe variations in the x-ray attenuation coefficients of biological tissues. This condition depends on the scattering angle of the EDXRD setup. For our particular setup, the rate was calculated with the scattering fluxes at the energy E_1 = 11.6 keV of the fibroglandular main peak (q=1.65 nm^{-1}) and the Mo-Kβ characteristic line E_2 = 19.88 keV. Using the equation (7) the logarithm of this rate can be expressed as:

$$ln\left(\frac{I_1}{I_2}\right) = A + B\,t \qquad (8)$$

where:

$$A = ln\left(\frac{I_{01}d\sigma_c(E_1)/d\Omega}{I_{02}d\sigma_c(E_2)/d\Omega}\right); \qquad B = \frac{(\mu_2-\mu_1)}{2}\left(\frac{1}{\cos 2\theta}-1\right)$$

It is not expected to observe variations in A between samples since the elemental composition of fibroglandular and neoplastic tissues are quite similar. However, the B factor should change appreciable between these two tissues taking higher negative values for neoplastic tissues. Then, the measurements of the rate I_1/I_2 and the sample thickness t would be employed to study variations in the slope B, that could be used to classify fibroglandular and malignant carcinomas.

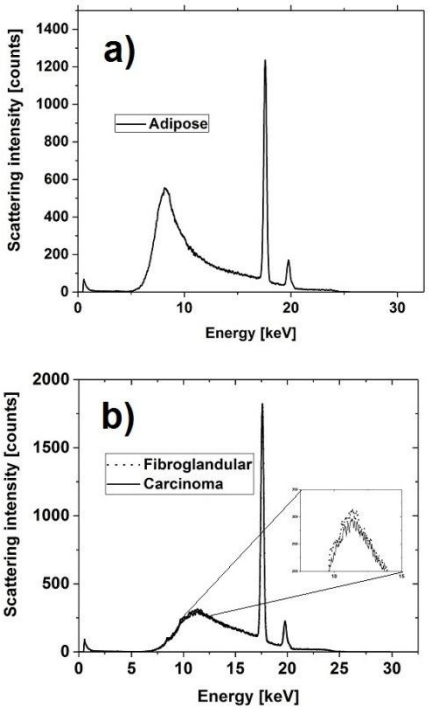

Figure 4: Typical scattering profiles for breast tissues measured with the microdiffractometer: a) adipose tissue, b) ductal carcinoma and fibroglandular samples with the same thickness. The inserted graph is an amplification of the slight differences between both patterns.

To test the linear dependence described by equation (8), PMMA phantoms were analyzed with the developed microdiffractometer. The scattering profiles were obtained for the four PMMA plates used before to test the thickness measurement method. The ordered pairs (t, ln (I_1/I_2)) obtained from the scattering profiles of PMMA plates were fit by a linear function. As shown in the Figure 5, the linear dependence was very well defined with low dispersion in the experimental points.

View Article Online
DOI: 10.1039/C9AY02187C

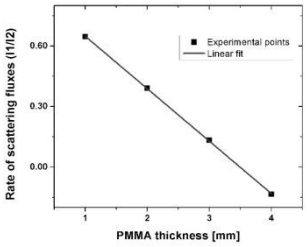

Figure 5: Rate of the scattering fluxes for PMMA at energies E_1=11.6keV and E_2=19.88keV versus PMMA thickness. Logarithm scale was used in the vertical axis. The low dispersion of the experimental points confirms the linear relation predicted by the model.

Once equation (8) was confirmed, fifteen fibroglandular samples were analyzed with the microdiffractometer and the ordered pairs (t, ln (I_1/I_2)) were obtained from the scattering profiles. The uncertainties for I_1 and I_2 were calculated assuming a Poisson statistical model for the registered counts. The linear fitting with the 95% confidence band is shown in Figure 6 a). Figure 6 b) shows the ordered pairs (t, ln (I_1/I_2)) obtained for ductal carcinomas. This Figure also shows the confidence band obtained in the linear fitting of the normal fibroglandular tissues which allows to see that the most ordered pairs of ductal carcinomas were clearly distinguished from normal fibroglandular tissues. This result shows that the evaluation of the x-ray attenuation in tissues samples by means of the equation (5) can be efficiently employed to develop a diagnostic model. The observed trend was broken when the samples presented considerable proportions of adipose tissue or microcalcifications. As a result, the highest efficiency in tissue differentiation was obtained by selecting the point of irradiation without such contributions. This selection can be precisely done thanks to the high spatial resolution of the spectrometer. Since the linear relation described by equation (8) for neoplastic and fibroglandular tissues have almost the same value for the ordinate A, the differences between both linear functions are manifested more clearly for larger thicknesses. In the experiments developed it was observed that for thicknesses around or higher than 2mm both linear relationships were distinguished properly.

It is important to highlight that a successful application of the proposed methodology requires a homogeneous tissue along the path of the incident and emergent beams. Points with inhomogeneities in depth should be avoided since they could produce a failure of the diagnostic model. However these kinds of points are difficult to recognize in the previous analysis of the sample by optical microscope. For those particular cases, the scan of the sample in depth initially employed to measure the sample thickness could also be used to identify possible variations in the x-ray attenuation coefficient. It should be determined with higher precision increasing the acquisition time of each step in order to detect subtle changes in the scattering intensity of the Mo-Kα line. The equation (5) is no longer able to precisely fit the experimental points since it was deduced under the hypothesis of uniform matter. Then discrepancies in the fitting model could be used as a signal of the presence of non uniform volume of analysis not suitable for the diagnostic model. The efficiency of this procedure was not tested in this work since inhomogeneities in depth were not observed in the set of samples available probably because the carcinomas were highly developed. Further research in this sense is under way in an extended set of samples.

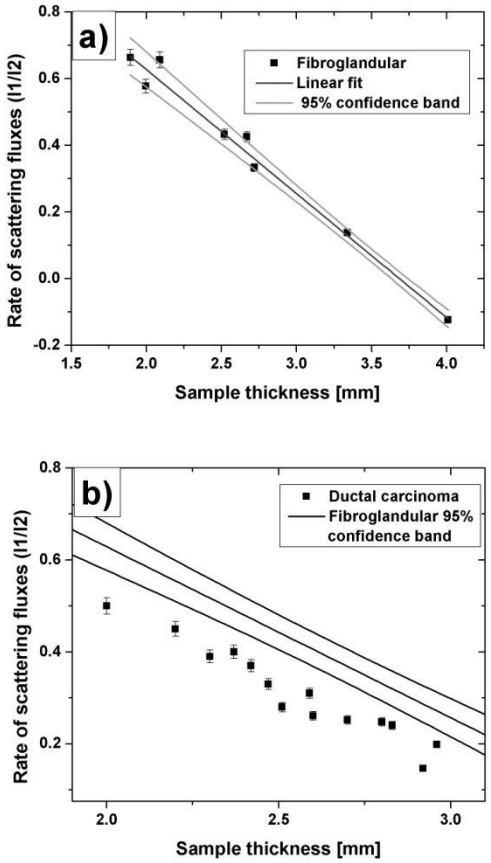

Figure 6: Rate of the scattering fluxes for breast tissues at energies E_1=11.6keV and E_2=19.88keV versus sample thickness with errors bars. Logarithm scale was used in the vertical axis. a) Linear fit of experimental points for fibroglandular tissues with the 95% confidence band. b) Experimental points for ductal carcinomas and the 95% confidence band of normal tissues.

Conclusions

In the present paper a dedicated confocal microdiffractometer has been employed to develop a deterministic diagnostic model of breast cancer. The model takes advantage of the high spatial resolution of the confocal setup to precisely determine the sample thickness and to select a homogeneous volume of analysis. Both characteristics were essential to properly

View Article Online
DOI: 10.1039/C9AY02183C

discriminate biological tissues with similar scattering profiles as fibroglandular and malignant carcinomas. In these particular cases, the higher x-ray attenuation of the neoplastic tissues was the key for the classification. It was clearly determined from the scattering profiles thanks to the application of the diffraction theory for scattering intensity in the description of the scattering fluxes. The proposed methodology could help to analyze biopsies in traditional histological labs with minimum training for operators.

Acknowledgements

This work was supported by the SECyT-UNC (grant 33620180100347CB) and CONICET from Argentina. The authors want thanks to Rocío Perez Sbarato for her assistance in the writing of the manuscript.

Notes and references

1 V. Kumar, A.K. Abbas, J.C. Aster. Robbins and Cotran Pathologic Basis of Disease, 9th Edition. Imprint of Saunders, Elsevier Inc., Amsterdam, 2015.
2 J. Kosanetzky, B. Knoerr, G. Harding, U. Neitzel. Med. Phys., 1987, 14, 526–32.
3 R. Speller. X-Ray Spectrom., 1999, 28, 244-250.
4 D.A. Bradley, K. Wells. Rad. Phys. Chem., 2013, 85,42–52.
5 G. Harding, B. Schreiber. Rad. Phys. Chem., 1999, 56, 229-245.
6 C. Sosa, A. Malezan, M. Poletti, R.D. Perez. Rad. Phys. Chem., 2017, 137, 125-129.
7 A. Tomal, I. Mazarro, E.M. Kakuno, M.E. Poletti. Rad. Measurements, 2010, 45, 1055-1059.
8 W. Malzer, B. Kanngieβer. 2005. Spectrochim. Acta B, 2005, 60, 1334-1341.
9 C. Sosa, H.J. Sánchez, C.A. Pérez, R.D. Perez. Nucl. Instr. and Meth. B, 2014, 319, 171–176.
10 H. Eba, Y. Kitakubo, S. Awaji, M. Takahashi. Nucl. Instr. and Meth. B, 2019, 456, 42–48.
11 F. Li, Z. Liu, T. Sun, Y. Ma, X. Ding. Food Control, 2015, 54, 120-125.
12 S. Clark. Cryst. Rev., 2002, 8, 57-92.
13 O.R. Oliveira, A.L.C. Conceição, D.M. Cunha, M.E. Poletti, C.A. Pela. J. of Rad. Res., 2008, 49, 527-532.
14 V. Stoytschew, M. Schulte-Borchers, I. Bozicevic Mihalica, R.D. Perez. Nucl. Instr. and Meth. B , 2016, 380, 99-102.
15 F. Salvat, J.M. Fernández-Varea. Metrologia, 2009, 46, S112–S138.
16 R.M. Moss, A.S. Amin, C. Crews, C.A. Purdie, L.B. Jordan, F. Lacoviello, A. Evans, R.D. Speller and S.J. Vinnicombe. Scientific Reports, 2017, 7, 12998.